Ginsenoside Rg1 attenuates inflammatory injury and apoptosis in autoimmune thyroiditis by reshaping the Notch1/Hes1–CDH2 axis

Nan Wang[1], Lin Chen[1,2], Yan Sun[1]*, Yongxia Xu[1]

[1]The First Affiliated Hospital of Anhui Medical University, China
[2]Anhui Public Health Clinical Center, China

Submitted: 13 December 2025; **Accepted:** 28 April 2026
Online publication: 20 July 2026

Arch Med Sci
DOI: https://doi.org/10.5114/aoms/221197

***Corresponding author:**
Yan Sun
The First Affiliated Hospital of Anhui Medical University China
E-mail: YyanSun22@outlook.com

Abstract

Introduction: This study aimed to determine whether ginsenoside Rg1(Rg1) alleviates inflammation and apoptosis in autoimmune thyroiditis (AIT) by remodeling the Notch1/Hes1 signaling pathway, and to evaluate the potential of this pathway as a therapeutic target.

Material and methods: Differentially expressed genes (DEGs) were identified from the GSE269497 bulk RNA-seq dataset and intersected with Notch1/Hes1 pathway gene sets to screen for candidate molecules. A protein–protein interaction network, CIBERSORT immune infiltration analysis, gene set enrichment analysis (GSEA), and gene set variation analysis (GSVA) were conducted to characterize CDH2-related immune and pathway features. Public GWAS/eQTL datasets were integrated using two-sample Mendelian randomization (MR) to evaluate the causal relationship between candidate genes and AIT risk. Single-cell RNA sequencing data from GSE163203 were used to analyze the cell-type-specific distribution of CDH2 in the thyroid microenvironment. *In vitro* validation was performed using CCK-8, RT-qPCR, and Western blot to assess cell viability, Notch1/Hes1 signaling, CDH2 levels, and apoptosis-related proteins.

Results: Transcriptomic analysis revealed disrupted Notch1/Hes1 signaling and significant upregulation of CDH2 in AIT. MR analysis indicated a positive causal relationship between genetically predicted CDH2 expression and AIT susceptibility. Elevated CDH2 expression correlated with reduced regulatory T-cell infiltration and enrichment of pro-inflammatory and stress-related pathways, including complement/coagulation, oxidative phosphorylation, and proteasome activation. *In vitro*, inflammatory stimulation inhibited Notch1/Hes1 signaling, shifted the Bcl-2/Bax–caspase axis toward apoptosis, and increased CDH2 expression. Rg1 treatment restored Notch1/Hes1 activation, increased Bcl-2 expression, reduced Bax and cleaved caspase-3 levels, suppressed CDH2 expression, and improved cell viability.

Conclusions: Rg1 reduces inflammatory apoptosis and tissue damage in thyroid follicular cells during autoimmune thyroiditis (AIT) by reshaping the Notch1/Hes1–CDH2 axis, thereby enhancing pro-survival signals while inhibiting CDH2-mediated abnormal adhesion and pro-inflammatory activation. The Notch1/Hes1–CDH2 axis may serve as a potential target for mechanism-guided adjuvant therapy in AIT.

Key words: autoimmune thyroiditis, Hashimoto's thyroiditis, ginsenoside Rg1, Notch1/Hes1, CDH2, Mendelian randomization, single-cell RNA sequencing, apoptosis, inflammation.

Introduction

Autoimmune thyroiditis (AIT), including Hashimoto's thyroiditis, is one of the most common organ-specific autoimmune diseases [1–3]. Its pathological hallmarks include chronic lymphocytic infiltration, the production of anti-thyroid autoantibodies, and progressive destruction of follicular structures, which may eventually lead to varying degrees of hypothyroidism [4]. Current treatment mainly relies on thyroid hormone replacement, which can correct hormonal deficiency but fails to halt immune-mediated tissue damage [5]. Moreover, mechanism-based interventions targeting early inflammatory responses and thyroid follicular cell (TFC) injury remain lacking [6]. Increasing evidence indicates that the pathogenesis and progression of AIT are not simply the result of immune cell attacks on the target organ but rather reflect a multifactorial imbalance involving immune cells, TFCs, stromal cells, and multiple signaling pathways [7, 8]. Among these, dysregulated apoptosis and amplified inflammatory responses play central roles in structural destruction and functional decline [9, 10]. Therefore, elucidating the key signaling networks driving TFC apoptosis and inflammatory injury, as well as identifying druggable molecular targets for precise regulation, is crucial to advancing AIT therapy from symptomatic hormone replacement toward mechanism-based intervention.

The Notch signaling pathway is a classical axis governing cell fate and tissue homeostasis, exerting context-dependent, bidirectional effects in immune differentiation, inflammatory responses, and tissue remodeling [11]. The Notch1/Hes1 axis participates in lymphocyte development and effector differentiation, as well as in maintaining the survival and regenerative balance of epithelial, endothelial, and stromal cells [12–14]. Depending on the microenvironment, it can act as either a pro-inflammatory/damaging or a protective/restorative signal. However, the specific function of Notch1/Hes1 in AIT remains unclear. Previous studies have mainly focused on immune cells, lacking systematic evidence regarding the role of Notch1/Hes1 in follicular epithelial cells and its integration with genetic susceptibility, adhesion remodeling, and apoptotic pathways. Ginsenoside Rg1 (Rg1), a representative active compound from Panax ginseng, has been proven to possess anti-inflammatory, antioxidant, anti-apoptotic, and tissue-protective effects [15]. It modulates cell fate and immune responses through multiple signaling cascades, such as PI3K/Akt, Nrf2, and NF-κB, and has demonstrated protective roles in cardiovascular, neurological, and metabolic disorders [16, 17]. However, in organ-specific autoimmune diseases such as AIT, studies to date on Rg1 have been largely empirical, focusing on its general anti-inflammatory and tissue-protective actions without establishing a detailed mechanistic framework supported by multi-omics and genetic evidence. Whether Rg1 can remodel local immune–structural interactions within the thyroid microenvironment through specific signaling nodes remains an open question.

Recent advances in multi-omics integration and causal inference have provided powerful tools to address such mechanistic gaps [18, 19]. Transcriptomic profiling, immune infiltration analysis, and single-cell RNA sequencing (scRNA-seq) enable the characterization of pathway expression patterns and immune microenvironment features at the tissue and cellular levels. Two-sample Mendelian randomization (MR) further allows causal evaluation of candidate molecular associations with AIT risk from a genetic perspective, overcoming the limitations of correlative analyses [20, 21]. Building upon these, combined with in vitro functional validation, a continuous mechanistic chain can be established from genetic susceptibility to transcriptional dysregulation, signaling imbalance, and pharmacological modulation. This study comprehensively conducted batch transcriptome analysis of GSE269497 and two-sample MR to identify and validate the key role of CDH2 in the Notch1/Hes1-related network. Simultaneously, it combined single-cell data from GSE163203, immune infiltration analysis, and GSEA/GSVA to delineate its corresponding cellular origin and inflammatory and metabolic characteristics. Based on this, functional validation was achieved in an inflammatory-stimulated Nthy-ori 3-1 cell model through Rg1 treatment, DAPT blockade, and siCDH2 intervention.

This study evaluated, from multiple perspectives, whether Rg1 alleviates AIT-related apoptosis and inflammatory damage by remodeling the Notch1/Hes1–CDH2 axis, and explored the feasibility of CDH2/Notch1/Hes1 as a potential precise intervention target.

Material and methods

Cell lines, reagents, and construction of an *in vitro* model of autoimmune thyroiditis

The human thyroid follicular epithelial cell line Nthy-ori 3-1 was obtained from the Cell Bank of the Chinese Academy of Sciences and cultured at 37°C in a humidified incubator with 5% CO_2. Cells were maintained in RPMI-1640 supplemented with 10% fetal bovine serum (FBS, Gibco) and 1% penicillin–streptomycin and were passaged at 70–80% confluence.

To establish an *in vitro* autoimmune thyroiditis (AIT)-like inflammatory injury model, cells were stimulated with a pro-inflammatory cytokine cocktail consisting of recombinant human TNF-α

(10 ng/ml) and IFN-γ (1000 U/ml) for 24 h to mimic the inflammatory microenvironment characteristic of AIT. These concentrations were selected based on published studies showing that TNF-α and IFN-γ can effectively induce inflammatory responses and injury-related changes in thyroid follicular epithelial cells [6]. Successful model establishment was defined by a significant reduction in cell viability and suppression of Notch1/Hes1 signaling compared with untreated controls.

Ginsenoside Rg1 (purity ≥ 98%; Solarbio, R8120) was dissolved in anhydrous DMSO to prepare a stock solution and used at a final working concentration of 40 μM. The concentration was selected with reference to published studies reporting cytoprotective effects of Rg1 in cell models over a micromolar concentration range, including evidence that concentrations up to 40 μM can improve cell viability without obvious cytotoxicity [6]; this was further confirmed by our preliminary dose–response assays, in which 40 μM produced the strongest protective effect without detectable toxicity (final DMSO concentration ≤ 0.1%).

To pharmacologically inhibit Notch signaling, the γ-secretase inhibitor DAPT (Selleckchem, S2215) was used at a concentration of 10 μM. Cells were pretreated with DAPT for 1 h prior to cytokine stimulation and maintained in the presence of DAPT throughout the 24 h treatment period.

For CDH2 knockdown experiments, small interfering RNAs (siRNAs) targeting human CDH2 (N-cadherin) were synthesized commercially.

siCDH2 (Sigma-Aldrich/Merck): Sense (5′–3′): GGCUUAUGGUGUGAUCUAUtt, Antisense (5′–3′): AUAGAUCACACCAUAAGCCtt.

A non-targeting scrambled siRNA was used as a negative control: siNC (Scrambled control): Sense (5′–3′): UUCUCCGAACGUGUCACGUtt, Antisense (5′–3′): ACGUGACACGUUCGGAGAAtt.

Cells were transfected with siRNAs at a final concentration of 50 nM using Lipofectamine 3000 (Invitrogen) according to the manufacturer's protocol. Transfection efficiency and knockdown effectiveness were verified by RT-qPCR and Western blot analysis 24–48 h after transfection.

Differential expression and pathway enrichment analysis

Bulk RNA-seq data (GSE269497) were downloaded from the Gene Expression Omnibus (GEO) database. Differential expression analysis between the AIT group (n = 5) and control group (n = 5) was performed in R (v4.2.1). Gene-level expression values were $\log_2$-transformed where appropriate. The limma workflow was applied (including voom transformation for count-based input when necessary), and differentially expressed genes (DEGs) were identified using the thresholds $|\log_2$ fold change$|$ > 0.586 and false discovery rate (FDR) < 0.05. Heatmaps and volcano plots were generated to visualize global expression patterns.

To identify Notch1/Hes1-related candidate genes, the DEG list was intersected with a predefined Notch signaling gene set. The reference Notch pathway gene sets were obtained from the Molecular Signatures Database (MSigDB), including Reactome and Hallmark Notch signaling collections. In addition, to specifically reflect the Notch1/Hes1 regulatory axis emphasized in this study, a curated Notch1/Hes1-related gene list was constructed by integrating canonical pathway components (NOTCH receptors, DLL/JAG ligands, RBPJ–MAML transcriptional complex members, γ-secretase complex components, and Hes/Hey downstream targets) with literature-supported Notch1/Hes1-associated genes. The complete list of genes included in this Notch1/Hes1-related core set is provided in Supplementary Table SI.

Protein–protein interaction (PPI) analysis of intersecting genes was performed using the STRING database (minimum interaction score ≥ 0.4), and the resulting network was visualized in R to identify highly connected nodes.

Mendelian randomization analysis

A two-sample Mendelian randomization (MR) analysis was performed using the TwoSampleMR framework to evaluate causal relationships between candidate gene expression and AIT risk. Exposure instruments (eQTL and/or pQTL variants) were extracted from publicly available summary-statistics resources (IEU OpenGWAS and deCODE Genetics Summary Statistics Portal). Instrumental variables were selected at genome-wide significance ($p < 5 \times 10^{-8}$) and pruned for linkage disequilibrium ($R^2 < 0.01$ within a 10,000 kb window). Variants strongly associated with known confounders were removed where applicable.

Outcome GWAS summary statistics for autoimmune thyroid disease were obtained from IEU OpenGWAS. Harmonization was performed to align effect alleles across exposure and outcome datasets. The inverse variance–weighted (IVW) method served as the primary estimator, with weighted median and MR-Egger as complementary approaches. Cochran's Q test assessed heterogeneity, while horizontal pleiotropy was evaluated using the MR-Egger intercept and funnel plot symmetry. Leave-one-out analyses were performed to examine robustness. Statistical significance was set at two-sided $p < 0.05$.

Immune infiltration analysis and GSEA/GSVA

Immune cell composition was estimated using CIBERSORT with the LM22 signature matrix.

The normalized expression matrix of GSE269497 was uploaded/processed in relative mode with 100 permutations, and quantile normalization was disabled for RNA-seq–based input. Only samples with deconvolution $p < 0.05$ were retained for downstream comparisons. Differences in the proportions of 22 immune cell subsets between AIT and control tissues were assessed, and correlations between CDH2 expression and key immune populations were evaluated using Pearson or Spearman correlation as appropriate.

For pathway characterization, samples were stratified into CDH2-high and CDH2-low groups using the median CDH2 expression. Gene set enrichment analysis (GSEA) was conducted using KEGG gene sets implemented in clusterProfiler with 1,000 permutations; pathways with |NES| > 1, nominal $p < 0.05$, and FDR < 0.25 were considered enriched. In parallel, gene set variation analysis (GSVA) was performed to compute pathway-level enrichment scores for each sample using the GSVA package.

Single-cell RNA sequencing analysis

Single-cell RNA sequencing data (GSE163203) were analyzed using Seurat (v4.3.0). Cells were filtered to remove low-quality data based on standard quality control metrics: < 200 genes detected per cell, > 6,000 genes detected per cell, and > 15% mitochondrial transcript content. The filtered data were normalized using LogNormalize (scaling factor 10,000) and scaled before dimensionality reduction. Highly variable genes were identified, and principal component analysis (PCA) was performed using the most variable features. A shared nearest neighbor graph was constructed using the first few principal components, followed by graph-based clustering. Low-dimensional embeddings were visualized using UMAP (or t-SNE).

Cell clusters were annotated using classic marker genes, including EPCAM/KRT8/KRT18 (follicular epithelial cells), COL1A1/DCN/LUM (stromal/mesenchymal cells), LST1/LYZ/C1QA (monocytes/macrophages), MS4A1/CD79A (B cells), and TRAC/CD3D (T cells). The expression distribution of CDH2 in the annotated cell types was visualized using FeaturePlot/DotPlot, and differences between major cell populations were compared.

CCK-8 cell viability assay

Cell viability was assessed using a CCK-8 assay (Beyotime, C0037). Nthy-ori 3-1 cells were seeded into 96-well plates at 5×10^3 cells/well (100 µl complete medium) and allowed to adhere overnight. Cells were then assigned to the following groups: control, inflammatory model (TNF-α + IFN-γ), model + Rg1, model + Rg1 + DAPT, model + siCDH2, and model + Rg1 + siCDH2. Unless otherwise stated, cytokine stimulation and drug interventions were maintained for 24 h. After treatment, 10 µl of CCK-8 reagent was added to each well and incubated for 1–2 h at 37°C. Absorbance was measured at 450 nm using a microplate reader. Blank wells containing medium plus CCK-8 were used for background subtraction. Cell viability was expressed as relative OD values normalized to the control group.

RT-qPCR assay

Total RNA was extracted using TRIzol reagent (Invitrogen) according to the manufacturer's protocol. RNA purity and concentration were determined by NanoDrop spectrophotometry. Reverse transcription was performed using a PrimeScript RT reagent Kit with gDNA Eraser (Takara, RR047A). Quantitative PCR was carried out using TB Green Premix Ex Taq II (Takara, RR820A) on a real-time PCR system.

Primer pairs targeting Notch1, Hes1, BCL2, BAX, CASP3, CDH2, and the reference gene GAPDH were synthesized commercially; all primer sequences are shown in Supplementary Table SII. The qPCR cycling program was as follows: initial denaturation at 95°C for 30 s, followed by 40 cycles of 95°C for 5 s and 60°C for 30 s, and a melt curve analysis to confirm amplification specificity. Relative gene expression was calculated using the $2^{-\Delta\Delta Ct}$ method with GAPDH as the internal control.

Western blot analysis

Cells were lysed in ice-cold RIPA buffer supplemented with protease and phosphatase inhibitor cocktails (final 1×). Lysates were clarified by centrifugation (12,000×g, 10–15 min, 4°C), and protein concentrations were determined using a BCA assay. Equal amounts of total protein (typically 20–30 µg per lane) were separated by SDS-PAGE (10–12% gels) and transferred onto PVDF membranes.

Membranes were blocked with 5% non-fat milk (or 5% BSA where appropriate) for 1 h at room temperature and incubated overnight at 4°C with primary antibodies. The following antibodies were used: Notch1 (CST, #3608), HES1 (CST, #11988), Bcl-2 (CST, #3498), Bax (CST, #5023), cleaved caspase-3 (CST, #9664), and N-cadherin/CDH2 (Abcam, ab18203). GAPDH or β-actin served as a loading control. Primary antibodies were typically diluted 1 : 1,000 in antibody dilution buffer, and HRP-conjugated secondary antibodies (anti-rabbit or anti-mouse IgG, as appropriate) were used at 1 : 5,000–1 : 10,000 for 1 h at room temperature. Bands were visualized using enhanced chemiluminescence (ECL) reagents and captured using

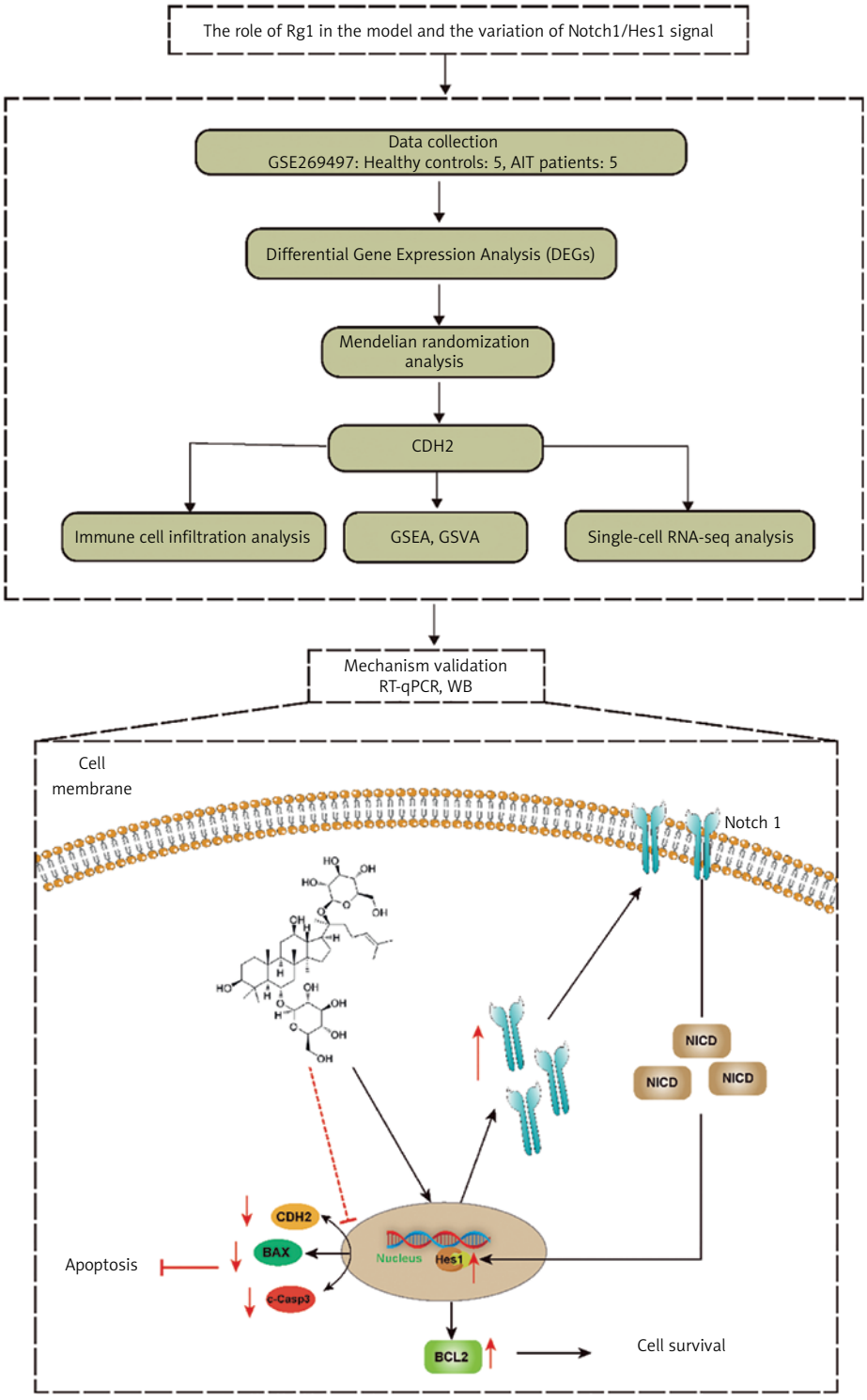

Figure 1. Workflow and mechanistic overview of ginsenoside Rg1 (Rg1) action in autoimmune thyroiditis (AIT). This study employed a multi-omics integrative strategy to systematically elucidate the molecular mechanisms of Rg1 in AIT. Using the GSE269497 transcriptomic dataset (five AIT and five control samples), differential expression, immune cell infiltration, and single-cell integration analyses were conducted to identify key genes associated with the Notch1/Hes1 signaling pathway. Candidate genes were further validated for causal associations with AIT phenotypes through Mendelian randomization (MR). Gene set enrichment analysis (GSEA) and gene set variation analysis (GSVA) revealed that CDH2 expression correlated with immune regulation and metabolic pathways. *In vitro* experiments confirmed that Rg1 activates the Notch1/Hes1 pathway, increases anti-apoptotic BCL2, and suppresses pro-apoptotic BAX and cleaved caspase-3 (c-Casp3). Rg1 also downregulates excessive CDH2 expression, mitigating inflammation driven by aberrant cell–cell adhesion. Collectively, multi-layered evidence demonstrates that Rg1 maintains cellular homeostasis and suppresses inflammatory apoptosis through modulation of the Notch1/Hes1–CDH2 axis, providing a molecular rationale for mechanism-based AIT therapy

a chemiluminescence imaging system. Densitometric quantification was performed in ImageJ, and target protein levels were normalized to the corresponding loading control.

Statistical analysis

All statistical analyses were performed using R (v4.2.1) and GraphPad Prism (v8.0). Data are presented as mean ± SD unless otherwise indicated. For *in vitro* experiments, each condition was evaluated using at least three independent biological replicates (n = 3), and statistical analyses were performed based on these independent experiments. Two-group comparisons were conducted using unpaired Student's t-test (or Mann–Whitney U test for non-normally distributed data). Multiple-group comparisons were performed using one-way ANOVA followed by Bonferroni or Tukey post hoc tests (or Kruskal–Wallis test with appropriate post hoc comparisons when data were not normally distributed). Correlation analyses were performed using Pearson or Spearman tests as appropriate. For multiple testing in omics analyses, the false discovery rate (FDR) was controlled using the Benjamini–Hochberg method. For Mendelian randomization analyses, statistical settings and sensitivity tests were as described above. A two-sided $p < 0.05$ was considered statistically significant.

Results

Rg1 modulates Notch1/Hes1 signaling activation in the autoimmune thyroiditis model

The overall workflow of this study is illustrated in Figure 1. In the *in vitro* autoimmune thyroiditis (AIT) model established by inflammatory stimulation of human thyroid epithelial cells (Nthy-ori 3-1), treatment with Rg1 significantly enhanced cell viability (Figure 2 A). CCK-8 assay results showed that the model group exhibited a marked decrease in cell viability, which was significantly restored following Rg1 treatment, indicating that Rg1 confers a protective effect against inflammation-induced cellular injury. RT-qPCR analysis demonstrated that the expression levels of Notch1 and Hes1 were markedly downregulated in the model group, suggesting suppression of the Notch1/Hes1 signaling pathway. After Rg1 intervention, the expression of both genes increased significantly, indicating reactivation of the pathway (Figure 2 B). These findings suggest that Rg1 may restore cellular homeostasis and mitigate inflammation-induced dysfunction by enhancing Notch1/Hes1 signaling.

Transcriptomic analysis reveals differentially expressed genes and dysregulation of the Notch1/Hes1 pathway in autoimmune thyroiditis

Based on the bulk RNA-seq dataset GSE269497 (five AIT samples and five control samples), a systematic transcriptomic analysis was performed to characterize molecular alterations in AIT. A total of 1,667 differentially expressed genes (DEGs) were identified, including 595 upregulated and 1,072 downregulated genes. Hierarchical clustering demonstrated clear separation between AIT and control samples (Figures 3 A, B). To further investigate Notch1/Hes1 pathway–associated abnormalities in AIT, the identified DEGs were intersected with a predefined Notch1/Hes1-related gene set derived from MSigDB Notch signaling collections and a curated Notch1/Hes1 core list (see Methods and Supplementary Table SI). This

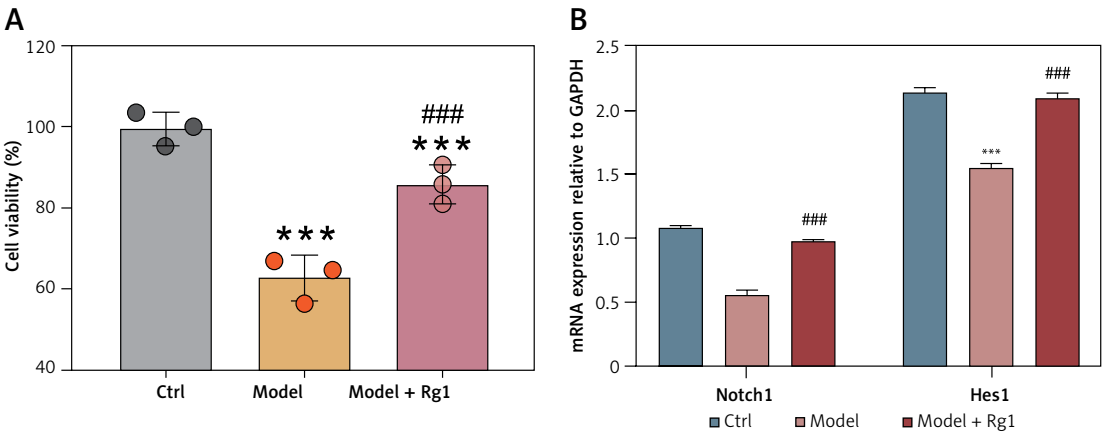

Figure 2. Regulation of the Notch1/Hes1 pathway by Rg1 in the AIT model. **A** – CCK-8 assay showing the effect of Rg1 treatment on Nthy-ori 3-1 cell viability following inflammatory stimulation with TNF-α and IFN-γ for 24 h. **B** – RT-qPCR analysis of Notch1 and Hes1 mRNA expression levels under different treatment conditions. Data are presented as mean ± SD from three independent experiments (n = 3). Statistical analysis was performed using one-way ANOVA followed by post hoc multiple comparisons. *$P < 0.05$, **$p < 0.01$, ***$p < 0.001$ versus control group; #$p < 0.05$, ##$p < 0.01$, ###$p < 0.001$ versus model group

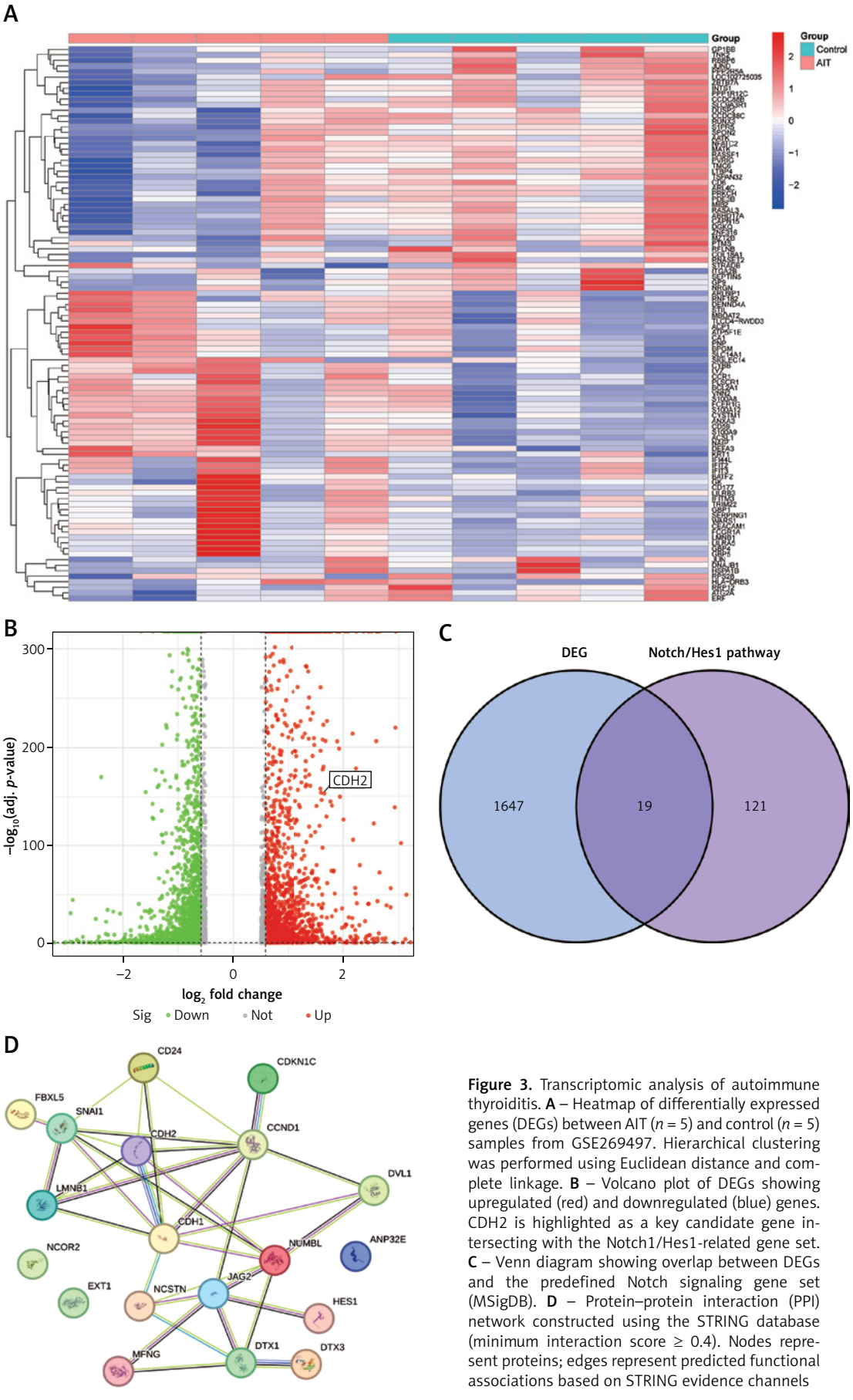

Figure 3. Transcriptomic analysis of autoimmune thyroiditis. **A** – Heatmap of differentially expressed genes (DEGs) between AIT ($n = 5$) and control ($n = 5$) samples from GSE269497. Hierarchical clustering was performed using Euclidean distance and complete linkage. **B** – Volcano plot of DEGs showing upregulated (red) and downregulated (blue) genes. CDH2 is highlighted as a key candidate gene intersecting with the Notch1/Hes1-related gene set. **C** – Venn diagram showing overlap between DEGs and the predefined Notch signaling gene set (MSigDB). **D** – Protein–protein interaction (PPI) network constructed using the STRING database (minimum interaction score ≥ 0.4). Nodes represent proteins; edges represent predicted functional associations based on STRING evidence channels

intersection yielded 19 overlapping candidate genes (Figure 3 C), suggesting coordinated dysregulation of Notch-related components in AIT tissues. A protein–protein interaction (PPI) network constructed using the STRING database revealed close interconnections among these intersecting genes (Figure 3 D), supporting the presence of a functionally integrated Notch1/Hes1-associated regulatory module in AIT.

Mendelian randomization analysis supports a causal relationship between CDH2 and autoimmune thyroiditis

To validate the potential causal relationship between CDH2 expression and autoimmune thyroiditis (AIT) risk, a two-sample Mendelian randomization (MR) analysis was performed using summary statistics from genome-wide association studies (GWAS). The inverse variance–weighted (IVW) method revealed a significant positive causal effect of CDH2 on AIT risk ($\beta = 0.272$, $p = 0.009$, OR = 1.312, 95% CI: 1.070–1.609). Consistent results were obtained using the weighted median (OR = 1.324, 95% CI: 1.041–1.685, $p = 0.022$) and MR-Egger (OR = 1.488, 95% CI: 1.058–2.092, $p = 0.048$) methods, indicating the robustness of the findings (Figure 4 A). Scatter and forest plots further confirmed that genetically predicted higher CDH2 expression was closely associated with increased AIT susceptibility (Figures 4 B, C). No significant horizontal pleiotropy was detected (MR-Egger intercept $p > 0.05$), and the funnel plot showed a symmetric distribution (Figure 4 D). Leave-one-out sensitivity analysis demonstrated the stability of the causal estimates (Figure 4 E), supporting the validity of the MR model. Collectively, these results indicate that higher genetically predicted CDH2 expression significantly increases the risk of developing AIT, suggesting CDH2 as an important causal mediator linking aberrant cell adhesion to autoimmune inflammatory responses.

Inflammatory features of CDH2 in autoimmune thyroiditis

Using the GSE269497 dataset, CIBERSORT-based immune infiltration analysis revealed notable differences in immune cell composition between AIT and control samples. Regulatory T-cell (Treg) populations were markedly reduced in AIT tissues (Figures 5 A, B), indicating impaired immune tolerance. Correlation analysis further demonstrated a significant negative relationship between CDH2 expression and Treg abundance ($r = -1$, $p = 0.017$) (Figure 5 C), suggesting that CDH2 may promote inflammation by weakening the immunosuppressive microenvironment.

To investigate the downstream molecular pathways involving CDH2, gene set enrichment analysis (GSEA) and gene set variation analysis (GSVA) were conducted. GSEA results showed that samples with high CDH2 expression were enriched in complement and coagulation cascades, oxidative phosphorylation, ubiquitin-mediated proteolysis, and proteasome pathways (Figure 5 D). The activation of these pathways reflects enhanced inflammatory amplification, oxidative stress, and disruption of protein homeostasis. Under AIT conditions, overexpression of CDH2 may compromise intercellular adhesion structures, leading to membrane signaling imbalance and inflammatory amplification. The positive correlation with complement activation implies that CDH2 may facilitate immune complex deposition and local immune activation, while enrichment of oxidative phosphorylation and ubiquitin system pathways suggests sustained metabolic stress and protein degradation activity. GSVA results further indicated that high CDH2 expression was accompanied by upregulation of oxidative metabolism–related pathways and significant downregulation of those associated with structural integrity and apoptosis balance (Figure 5 E).

Single-cell transcriptomic validation reveals cell type–specific expression of CDH2 in autoimmune thyroiditis

Single-cell RNA sequencing (scRNA-seq) analysis based on the GSE163203 dataset revealed substantial cellular heterogeneity within autoimmune thyroiditis (AIT) tissues (Figures 6 A, B). The expression of CDH2 exhibited clear cell type–specific distribution, being predominantly enriched in epithelial cells, stromal/mesenchymal cells, and macrophages, while showing low expression in lymphoid lineages, including naïve B and T cells. Notably, CDH2 expression was higher in M1-type macrophages compared with M0-type macrophages, suggesting a close association between CDH2 and pro-inflammatory activation states.

Experimental validation confirms that Rg1 inhibits apoptosis by regulating the Notch1/Hes1–CDH2 axis

CCK-8 assay results demonstrated that Rg1 treatment significantly enhanced the viability of Nthy-ori 3-1 cells ($p < 0.001$), whereas co-treatment with the γ-secretase inhibitor DAPT markedly reduced this effect, indicating that the protective action of Rg1 depends on the integrity of the Notch signaling pathway. Cell viability in the siCDH2 group was higher than that in the model group but lower than in the Rg1-treated group, while the combined Rg1 + siCDH2 treatment pro-

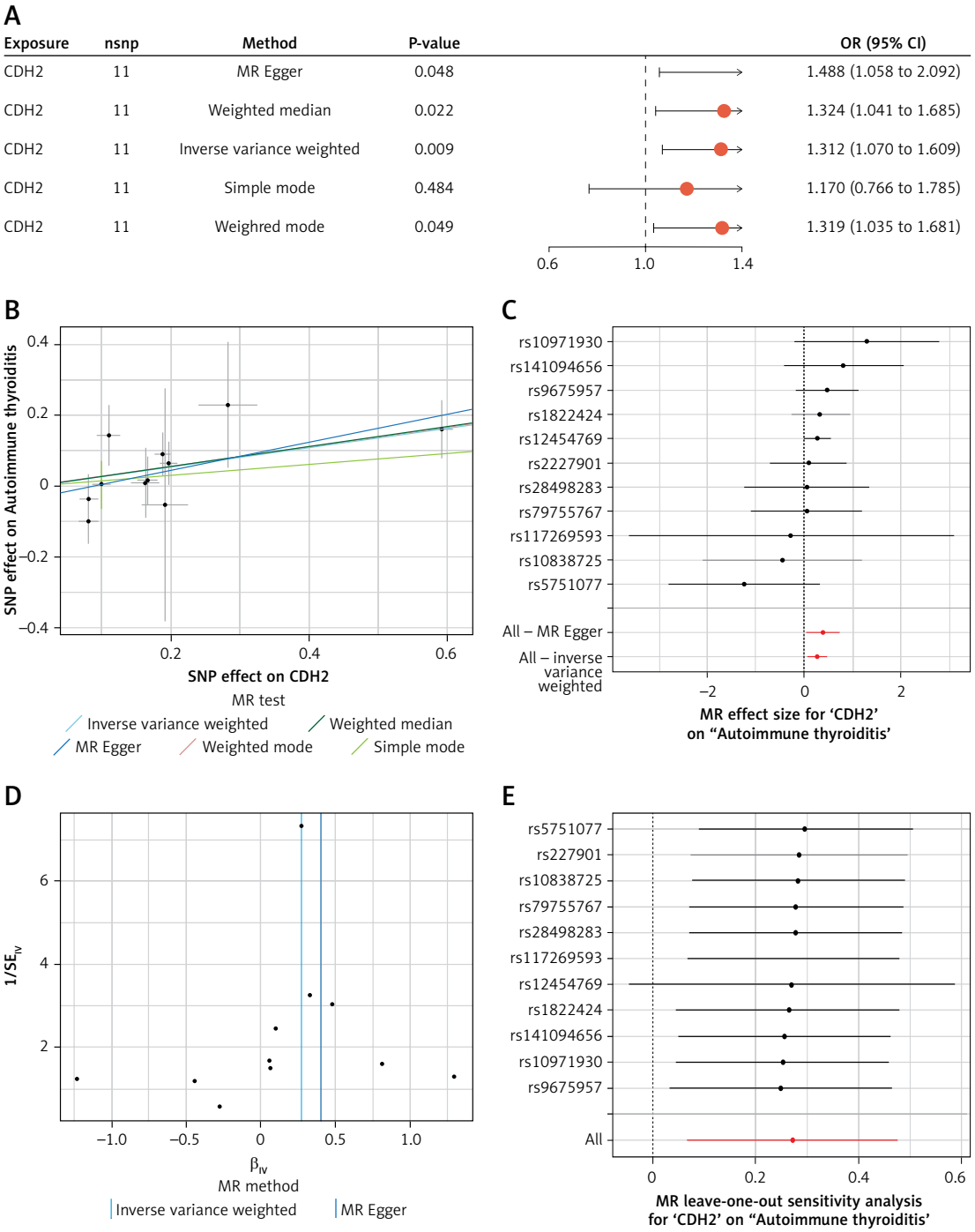

Figure 4. Mendelian randomization analysis of CDH2 and autoimmune thyroiditis. **A** – Forest plot of causal effects of CDH2 on AIT under different MR models. **B** – Scatter plot showing the direction of effects for 11 SNPs associated with CDH2 expression and AIT risk. **C** – Forest plot of individual SNP effect sizes with 95% confidence intervals. **D** – Symmetric funnel plot indicating no significant horizontal pleiotropy. **E** – Leave-one-out sensitivity analysis confirming result stability

duced the strongest recovery, approaching control levels (Figure 7 A).

RT-qPCR results (Figure 7 B) showed that Rg1 significantly upregulated Notch1 and Hes1 mRNA expression, while DAPT partially reversed this effect, confirming that Rg1-induced activation of the Notch1/Hes1 pathway is dependent on γ-secretase–mediated cleavage. Upon CDH2 silencing, Notch1 and Hes1 expression levels were intermediate between those in the Rg1 and DAPT groups, suggesting that adhesion signaling exerts a synergistic role in regulating Notch activation.

Regarding apoptosis-related genes, Rg1 treatment markedly increased anti-apoptotic BCL2

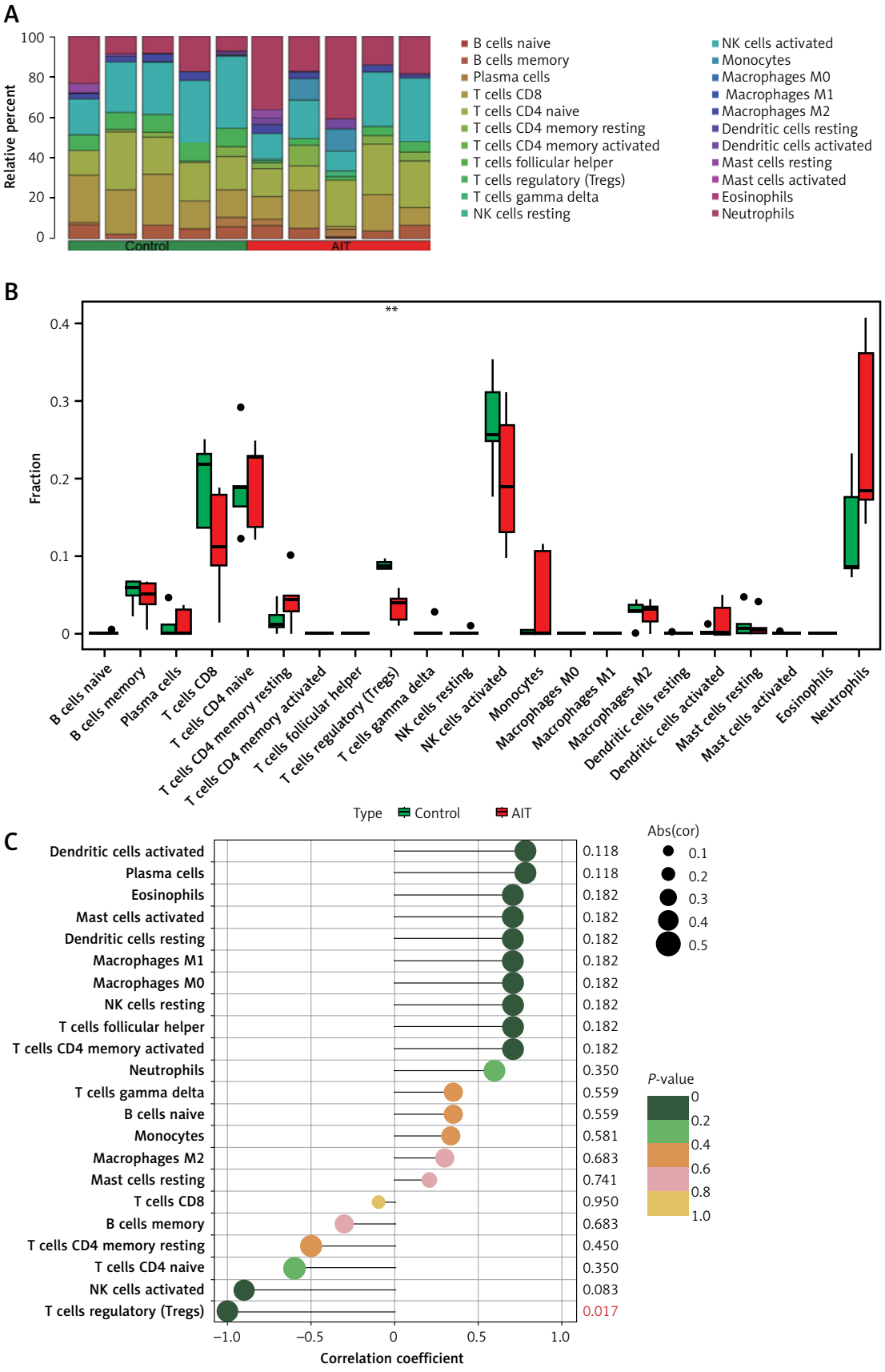

Figure 5. Immune correlations and functional enrichment of CDH2. **A** – CIBERSORT-based estimation of immune cell composition. **B** – Boxplot comparing immune cell subsets between AIT and control samples. **C** – Correlation analysis between CDH2 expression and selected immune cell populations

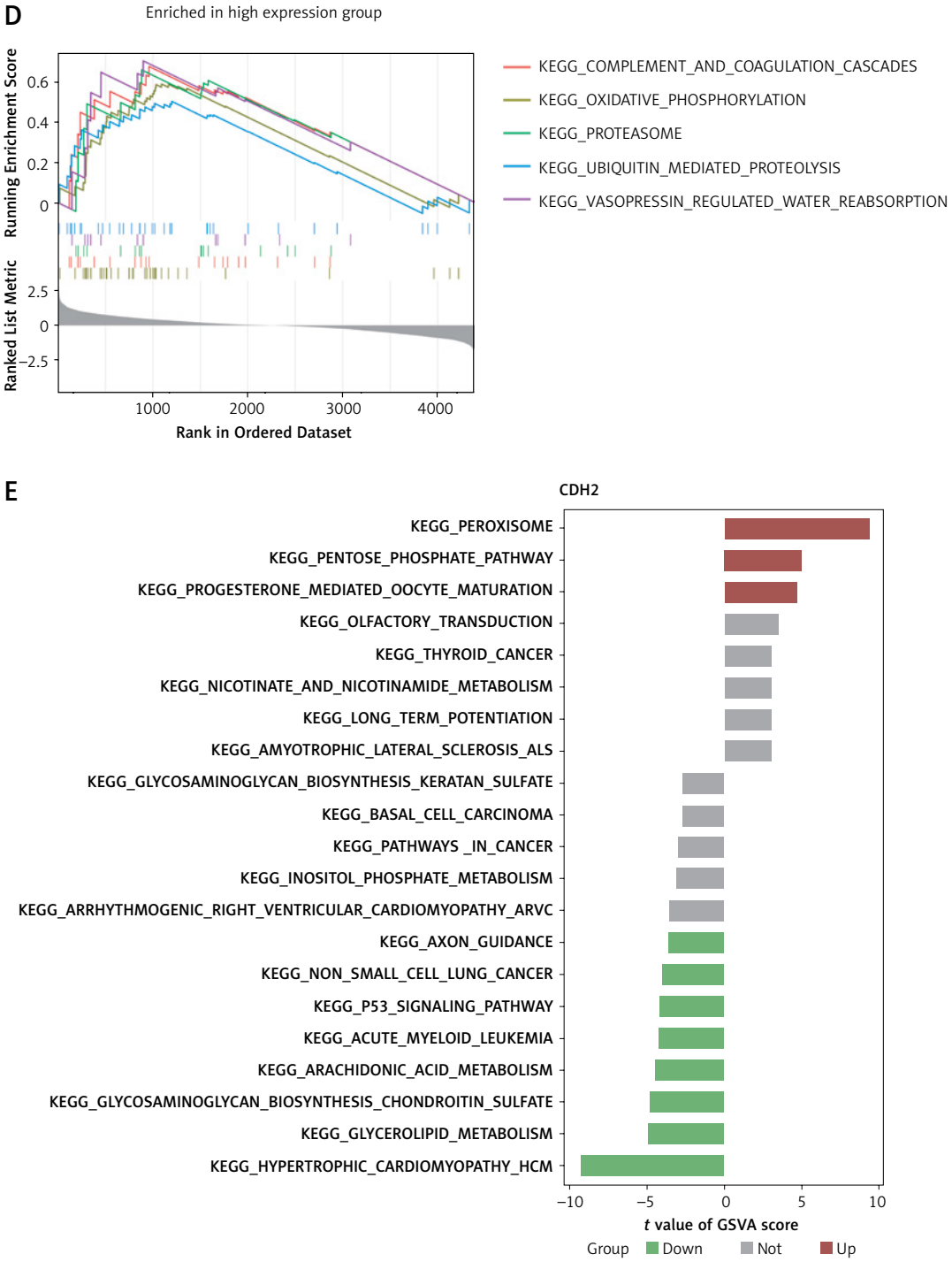

Figure 5. Cont. **D** – Gene set enrichment analysis (GSEA) showing pathways enriched in CDH2-high samples. **E** – GSVA analysis displaying pathway-level enrichment scores associated with CDH2 expression. Statistical comparisons were performed using one-way ANOVA or appropriate correlation tests. Significance thresholds are indicated in each panel

expression while decreasing pro-apoptotic BAX and cleaved caspase-3 levels, indicating a strong anti-apoptotic effect. Co-treatment with DAPT reduced BCL2 expression and restored BAX and c-Casp3 levels, further confirming that the effect is dependent on Notch1/Hes1 signaling. In the siCDH2 group, BCL2 remained elevated while BAX and c-Casp3 were significantly reduced, suggesting that CDH2 suppression enhances the anti-apoptotic potential of Rg1.

Western blot analysis yielded results consistent with mRNA expression (Figures 7 C, D). Compared to the control group, Rg1 treatment upregulated Notch1 and Hes1 protein levels, while DAPT par-

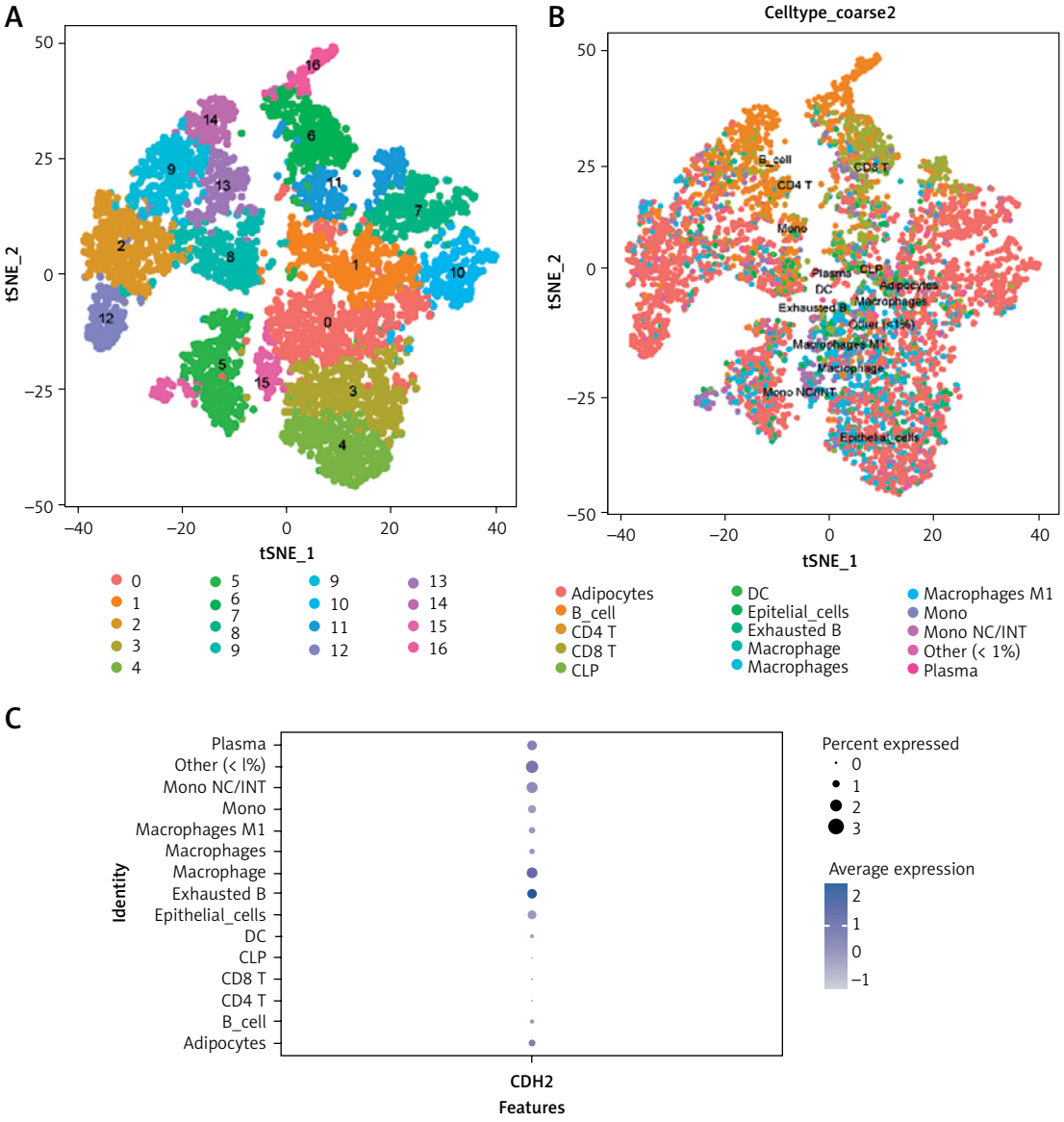

Figure 6. Cell type–specific expression of CDH2 in AIT based on single-cell RNA sequencing. **A** – t-SNE clustering of single-cell transcriptomic data from the GSE163203 dataset. **B** – Cell type annotation across major thyroid cell populations. **C** – Distribution of CDH2 expression across different cell clusters

tially reversed these increases. Rg1 also significantly elevated Bcl-2 expression and reduced Bax and cleaved caspase-3 levels; these changes were partially reversed by DAPT, reinforcing the notion that Rg1 acts through Notch1/Hes1 pathway activation. Similarly, CDH2 knockdown decreased CDH2 expression and maintained a higher Bcl-2/Bax ratio, implying that Rg1 may achieve self-limited protection by attenuating CDH2-mediated adhesion signaling and balancing Notch pathway activation intensity.

Taken together, these findings indicate that Rg1 reduces inflammatory apoptosis by activating the Notch1/Hes1 signaling pathway and downregulating CDH2 expression, thereby maintaining equilibrium within the Bcl-2/Bax–caspase axis. The proposed mechanism (Figure 7 E) illustrates that Rg1 mitigates aberrant intercellular adhesion and suppresses pro-inflammatory signal amplification through modulation of the Notch1/Hes1–CDH2 axis, ultimately protecting thyroid cells from immune-mediated injury.

Discussion

AIT, including Hashimoto's thyroiditis and related subtypes, is one of the most prevalent organ-specific autoimmune disorders [22–24]. It is characterized by persistent lymphocytic infiltration, production of anti-thyroid autoantibodies, and progressive follicular destruction, ultimately leading to hypothyroidism [25]. Current clinical management primarily relies on thyroid hormone replacement therapy, which corrects hormonal

deficiency but does not effectively reverse or halt immune-mediated tissue damage. Furthermore, there remains a lack of mechanistically validated, targeted therapeutic approaches. This study, through multi-omics integration, genetic causal inference, and in vitro functional validation, demonstrated that ginsenoside Rg1 alleviates apoptosis and inflammatory injury associated with AIT, in which the Notch1/Hes1–CDH2 axis plays a critical regulatory role. Transcriptomic and functional findings revealed that under AIT conditions, the Notch1/Hes1 signaling pathway is dysregulated, the Bcl-2/Bax–caspase cascade shifts toward a pro-apoptotic pattern, and CDH2 is aberrantly upregulated, closely linked to inflammatory amplification and structural disruption. Rg1

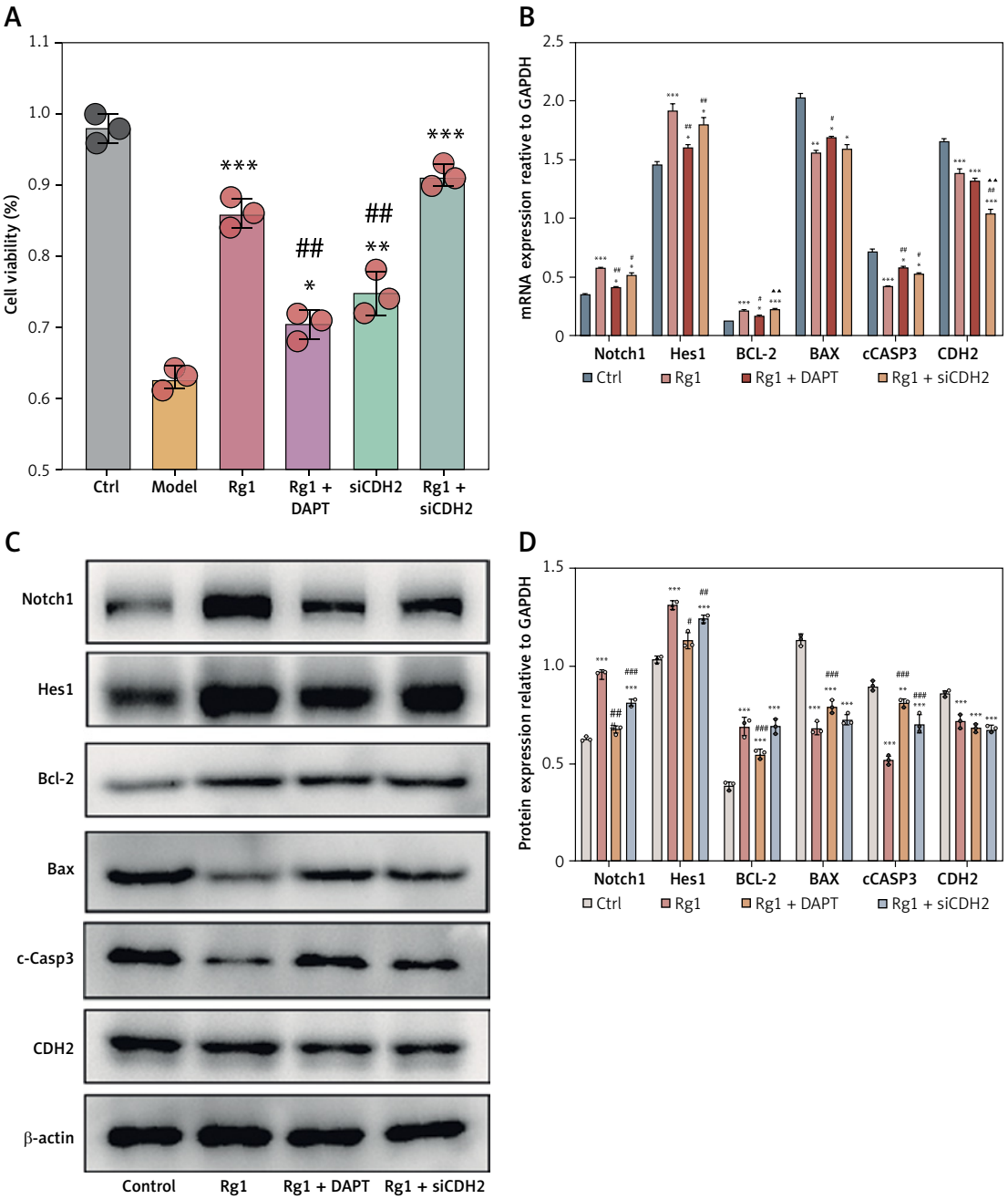

Figure 7. Experimental validation of Rg1-mediated apoptosis inhibition via the Notch1/Hes1–CDH2 axis. **A** – CCK-8 assay showing cell viability under different treatment conditions. **B** – RT-qPCR analysis of Notch1, Hes1, CDH2, BCL2, and BAX expression. **C** – Representative Western blot images of Notch1, HES1, CDH2, Bcl-2, Bax, and cleaved caspase-3, with GAPDH as loading control. **D** – Densitometric quantification of Western blot band intensities normalized to GAPDH. Data are presented as mean ± SD from three independent experiments (n = 3). Statistical analysis was performed using one-way ANOVA with post hoc testing. $^{*}P < 0.05$, $^{**}P < 0.01$, $^{***}P < 0.001$ versus model group; $^{\#}P < 0.05$, $^{\#\#}P < 0.01$, $^{\#\#\#}P < 0.001$ versus Rg1 group

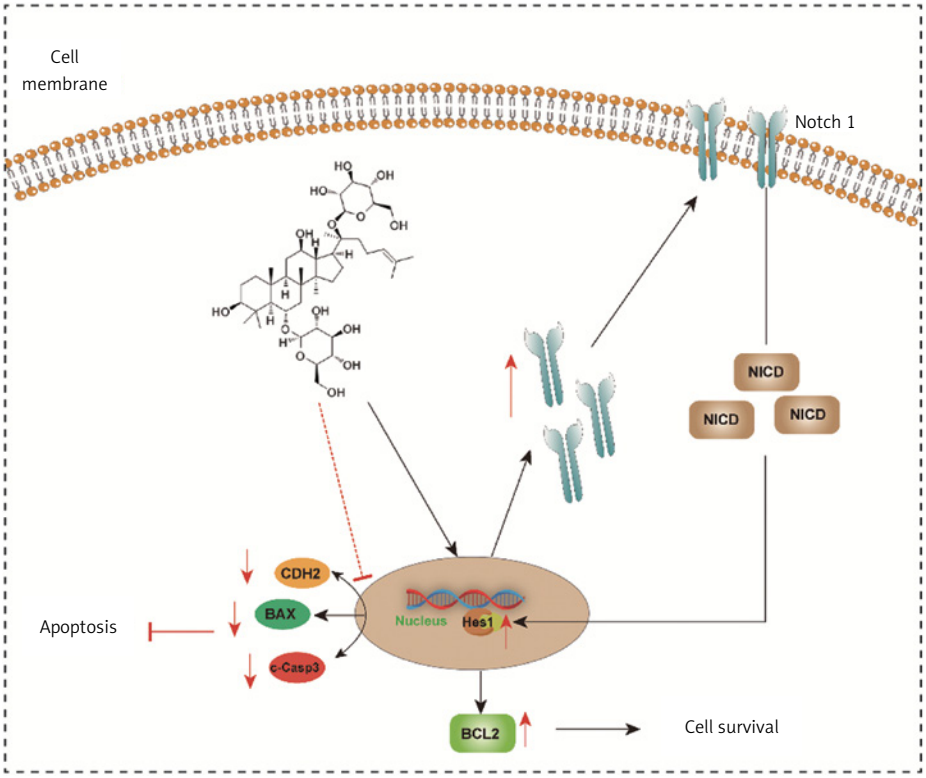

Figure 7. Cont. **E** – Proposed mechanistic model illustrating Rg1-mediated restoration of Notch1/Hes1–CDH2 axis balance. Data are presented as mean ± SD from three independent experiments (n = 3). Statistical analysis was performed using one-way ANOVA with post hoc testing. $^{*}P < 0.05$, $^{**}P < 0.01$, $^{***}P < 0.001$ versus model group; $^{\#}P < 0.05$, $^{\#\#}P < 0.01$, $^{\#\#\#}P < 0.001$ versus Rg1 group

treatment restored and enhanced Notch1/Hes1 pathway activity, suppressed CDH2 expression, remodeled the Bcl-2/Bax–caspase balance, and significantly improved cell viability. These findings suggest that Rg1 mitigates AIT-related cellular imbalance by simultaneously modulating signaling and adhesion nodes within the inflammatory microenvironment.

Ginsenoside Rg1, a prototypical active triterpenoid saponin isolated from Panax ginseng, possesses a well-defined chemical structure and an established safety profile [26]. Previous studies have confirmed its multifaceted roles, including anti-inflammatory, antioxidant, anti-apoptotic, and cytoprotective effects, mediated through the PI3K/Akt, Nrf2, and NF-κB pathways [17, 27, 28]. Rg1 has demonstrated broad protective actions in cardiovascular, neurological, and metabolic disorders. However, within organ-specific autoimmune diseases such as AIT, its effects have largely remained at the empirical or phenomenological level, lacking mechanistic elucidation supported by multi-omics and genetic evidence. In the present study, we observed that inflammatory stimulation of Nthy-ori 3-1 thyroid cells suppressed Notch1/Hes1 signaling and placed cells at high risk of apoptosis. Rg1 treatment markedly upregulated Notch1 and Hes1 expression, increased anti-apoptotic BCL2, reduced BAX and cleaved caspase-3, and restored cellular viability. The partial reversal of these effects by the Notch pathway inhibitor DAPT further confirmed that the protective activity of Rg1 depends on intact Notch1/Hes1 signaling. These observations align with previous reports describing the anti-apoptotic and tissue-protective properties of Rg1 across multiple pathophysiological contexts.

CDH2 (N-cadherin) has traditionally been recognized as a structural protein mediating cell–cell adhesion and participating in epithelial–mesenchymal transition (EMT) and tissue remodeling [29, 30]. It has been extensively studied in the contexts of tumor invasion, fibrosis, and vascular pathology, yet systematic investigation in autoimmune thyroiditis (AIT) has been lacking [31, 32]. In this study, multi-omics integration, Mendelian randomization, and immune infiltration analyses collectively revealed that CDH2 was markedly upregulated in AIT tissues. Genetically predicted CDH2 expression showed a robust positive causal association with AIT risk. High CDH2 expression correlated strongly with reduced regulatory T-cell (Treg) infiltration and enrichment of pro-inflammatory and stress-related pathways, including complement and coagulation cascades, oxidative phosphorylation, and proteasome activity.

Single-cell transcriptomic analysis further demonstrated that CDH2 was primarily enriched in follicular epithelial cells, stromal/mesenchymal cells, and pro-inflammatory macrophages, whereas its expression was relatively low in B and T lymphocytes. These findings suggest that CDH2 may function by modulating adhesion and activation processes in structural and innate immune cells, thereby shaping a pro-inflammatory microenvironment, rather than acting directly as an adaptive immune effector molecule [33]. Together, the evidence indicates that CDH2 is not merely a bystander marker of tissue injury but a pivotal hub that amplifies inflammation and bridges structural disruption with signaling imbalance.

The *in vitro* results provided functional support for this hypothesis. Rg1 treatment significantly downregulated CDH2 expression, while CDH2 knockdown alone reduced apoptosis and partially restored cellular protection. Combined Rg1 and siCDH2 treatment further enhanced cell viability, approaching control levels. This suggests that suppression of CDH2-mediated aberrant adhesion and contact-dependent signaling contributes to alleviating inflammatory injury and that part of Rg1's protective effect operates through this adhesion–signaling axis.

Recent studies have emphasized that immune dysregulation in chronic inflammatory and autoimmune diseases is not solely driven by effector T-cell activation but also by impairment of inhibitory immune circuits. Inhibitory NK cell receptor dynamics have been shown to modulate antiviral and chronic inflammatory responses, highlighting the importance of balanced inhibitory signaling in preventing excessive immune activation [34]. Likewise, $CD8^+$ suppressor T lymphocytes have been reported to exert non-antigen-specific regulatory functions in chronic inflammatory diseases, contributing to immune homeostasis and tissue protection [35]. In the context of AIT, diminished regulatory T-cell infiltration observed in our analysis may represent only one aspect of a broader disruption of immunosuppressive networks. Upregulation of CDH2 and dysregulation of the Notch1/Hes1 axis may further contribute to sustaining a pro-inflammatory microenvironment insufficiently restrained by inhibitory NK and $CD8^+$ suppressor mechanisms. These observations underscore the complexity of immune–structural cell interactions in AIT and support the concept that restoring signaling balance may help reestablish immune tolerance.

Integrating the multi-omics and MR findings, a mechanistic model can be proposed: in AIT, CDH2 upregulation leads to remodeling of intercellular adhesion structures, promoting dysregulated activation of Notch and related inflammatory pathways, thereby aggravating follicular structural destruction and apoptosis. Rg1 counteracts these effects by moderately activating the Notch1/Hes1 pathway while simultaneously suppressing CDH2 expression, shifting local signaling from a pro-inflammatory and pro-apoptotic state toward a balanced, homeostatic mode. This dual regulation ultimately restores follicular epithelial cell integrity and reestablishes microenvironmental equilibrium.

The findings of this study suggest that AIT is not a simple, linear process of lymphocyte-mediated organ attack but rather a multifactorial imbalance involving structural cells, innate immune cells, and adhesion/signaling molecules acting in concert. Within this network, the Notch1/Hes1 pathway contributes to cellular protection through moderate activation under specific microenvironmental conditions, while excessive or dysregulated signaling drives injury. The essential role of Rg1 is to recalibrate both the intensity and direction of Notch1/Hes1–CDH2 axis activity, restoring an optimal homeostatic window. This insight provides a theoretical foundation for more precise therapeutic targeting of Notch-related pathways and highlights CDH2 as a novel molecule with pharmacological relevance. Accordingly, CDH2 and molecules within the Notch1/Hes1–Bcl-2/Bax–caspase axis may serve as potential biomarkers for assessing inflammatory activity, predicting structural damage, and monitoring treatment response, thereby facilitating stratified and individualized management of AIT.

As a natural compound with a well-established pharmacological profile and favorable safety record, Rg1 could be considered a potential adjunct or protective intervention in AIT. It merits further evaluation in standardized dosage regimens and combination strategies. Furthermore, focusing on CDH2 – a critical node linking adhesion abnormalities with Notch/inflammatory amplification – may open new avenues for developing targeted therapies along the adhesion–signaling–microenvironment axis.

Nevertheless, this study has certain limitations. The multi-omics and Mendelian randomization analyses were based on publicly available datasets, and their interpretability may be influenced by limited sample sizes and population heterogeneity. Independent cohort validation is therefore required. The in vitro model primarily utilized Nthy-ori 3-1 cells, which, although capable of mimicking inflammation-induced follicular cell injury, cannot fully recapitulate the complexity of the AIT immune network and tissue microenvironment. Rg1 likely acts on multiple signaling pathways; however, this study focused specifically on the Notch1/Hes1–CDH2 axis, leaving its broader mechanistic landscape to be further explored.

In addition, whether CDH2 directly interacts with Notch receptors or the γ-secretase complex, and how these molecular interactions are spatially organized, remains to be experimentally clarified. Future studies should employ AIT animal models and clinical samples to systematically evaluate the long-term protective effects of Rg1 on thyroid structure and function, validate the diagnostic and prognostic value of CDH2/Notch-related biomarkers, and dissect the dynamic interplay among adhesion, signaling, and immunity at higher resolution. These efforts will lay the groundwork for translating the mechanistic framework proposed here into feasible and effective therapeutic strategies for AIT.

An important translational implication of our findings is whether pharmacogenomic strategies could help identify patients who are more likely to benefit from mechanism-guided adjuvant therapy. In immune-mediated diseases such as psoriasis and psoriatic arthritis, host genetic variation has been shown to influence therapeutic responses to biologic agents. For instance, TNF-α gene polymorphisms have been associated with disease susceptibility and response to etanercept treatment, highlighting the role of pharmacogenomics in therapeutic stratification [36, 37]. Although Rg1 is a natural compound rather than a biologic agent, a similar precision-medicine framework may be applicable in autoimmune thyroiditis. In the future, molecular features related to the Notch1/Hes1–CDH2 axis may help identify subgroups of patients with distinct inflammatory or apoptotic profiles who are more likely to benefit from Rg1-based adjunctive therapy.

In conclusion, through a combination of multi-omics analysis, Mendelian randomization, single-cell transcriptomics, and *in vitro* functional experiments, this study systematically elucidated the protective role and molecular basis of ginsenoside Rg1 in autoimmune thyroiditis (AIT). The results showed that under AIT conditions, imbalance of the Notch1/Hes1 pathway and abnormal upregulation of CDH2 were closely associated with follicular structural damage, impaired immune tolerance, and amplified inflammation. Rg1 alleviated these pathological changes by regulating the Notch1/Hes1–CDH2 axis, increasing Notch1/Hes1 expression, restoring balance in the Bcl-2/Bax–caspase apoptotic pathway, and reducing CDH2-mediated abnormal adhesion signaling, thereby decreasing inflammatory apoptosis and tissue injury in thyroid follicular cells.

Acknowledgments

Nan Wang and Lin Chen made equal contributions.

Funding

Key Project of Natural Science Research of Anhui Provincal Higher Education Institutions in 2023.

Ethical approval

Not applicable.

Conflict of interest

The authors declare no conflict of interest.

References

1. Piticchio T, Frasca F, Malandrino P, et al. Effect of gluten-free diet on autoimmune thyroiditis progression in patients with no symptoms or histology of celiac disease: a meta-analysis. Front Endocrinol 2023; 14: 1200372.
2. Ragusa F, Fallahi P, Elia G, et al. Hashimotos' thyroiditis: epidemiology, pathogenesis, clinic and therapy. Best Pract Res Clin Endocrinol Metab 2019; 33: 101367.
3. Ralli M, Angeletti D, Fiore M, et al. Hashimoto's thyroiditis: an update on pathogenic mechanisms, diagnostic protocols, therapeutic strategies, and potential malignant transformation. Autoimmun Rev 2020; 19: 102649.
4. Weetman AP. An update on the pathogenesis of Hashimoto's thyroiditis. J Endocrinol Invest 2021; 44: 883-90.
5. Martinez Quintero B, Yazbeck C, Sweeney LB. Thyroiditis: evaluation and treatment. Am Fam Physician 2021; 104: 609-17.
6. Caturegli P, De Remigis A, Rose NR. Hashimoto thyroiditis: clinical and diagnostic criteria. Autoimmun Rev 2014; 13: 391-7.
7. Ding H, Qin J, Liu Z, et al. Mesenchymal stem cells alleviate autoimmune thyroiditis by modulating macrophage phenotypes and through influencing the STING pathway. Tissue Cell 2024; 91: 102596.
8. Kimura H, Caturegli P. Chemokine orchestration of autoimmune thyroiditis. Thyroid 2007; 17: 1005-11.
9. Mo K, Chu Y, Liu Y, et al. Targeting hnRNPC suppresses thyroid follicular epithelial cell apoptosis and necroptosis through m(6)A-modified ATF4 in autoimmune thyroid disease. Pharmacol Res 2023; 196: 106933.
10. Zhao Z, Li J, Song N, et al. Buzhong Yiqi decoction improves inflammation and oxidative damage in autoimmune thyroiditis by inhibiting apoptosis via the SIRT1-Mediated Nrf2/NF-κB axis. J Ethnopharmacol 2025; 351: 119967.
11. Zhou B, Lin W, Long Y, et al. Notch signaling pathway: architecture, disease, and therapeutics. Signal Transduct Target Ther 2022; 7: 95.
12. Lin YW, Li XX, Fu FH, et al. Notch1/Hes1-PTEN/AKT/IL-17A feedback loop regulates Th17 cell differentiation in mouse psoriasis-like skin inflammation. Mol Med Rep 2022; 26: 223.
13. Wang L, Lai S, Zou H, et al. Ischemic preconditioning/ischemic postconditioning alleviates anoxia/reoxygenation injury via the Notch1/Hes1/VDAC1 axis. J Biochem Mol Toxicol 2022; 36: e23199.
14. Lu Y, Li SY, Lou H. Patchouli alcohol protects against myocardial ischaemia-reperfusion injury by regulating the Notch1/Hes1 pathway. Pharm Biol 2022; 60: 949-57.

15. Yang SJ, Wang JJ, Cheng P, et al. Ginsenoside Rg1 in neurological diseases: from bench to bedside. Acta Pharmacol Sin 2023; 44: 913-30.
16. Tang BL, Liu Y, Zhang JL, et al. Ginsenoside Rg1 ameliorates hypoxia-induced pulmonary arterial hypertension by inhibiting endothelial-to-mesenchymal transition and inflammation by regulating CCN1. Biomed Pharmacother 2023; 164: 114920.
17. Tian G, Li J, Zhou L. Ginsenoside Rg1 regulates autophagy and endoplasmic reticulum stress via the AMPK/mTOR and PERK/ATF4/CHOP pathways to alleviate alcohol-induced myocardial injury. Int J Mol Med 2023; 52: 56.
18. Ning L, Zhou YL, Sun H, et al. Microbiome and metabolome features in inflammatory bowel disease via multi-omics integration analyses across cohorts. Nat Commun 2023; 14: 7135.
19. He X, Liu X, Zuo F, et al. Artificial intelligence-based multi-omics analysis fuels cancer precision medicine. Semin Cancer Biol 2023; 88: 187-200.
20. Chen Z, Wang Y, Xu Y. Genetic association between autoimmune thyroiditis and microscopic polyangiitis: a two-sample Mendelian randomization study. Medicine 2024; 103: e40827.
21. Zhang Q, Lan X. Assessment of causal association between autoimmune thyroiditis and thyroid cancer: a Mendelian randomization study. Medicine 2025; 104: e41633.
22. Vargas-Uricoechea H. Molecular mechanisms in autoimmune thyroid disease. Cells 2023; 12: 918.
23. Mogahed EA, Soliman HM, Morgan DS, et al. Prevalence of autoimmune thyroiditis among children with autoimmune hepatitis. Ital J Pediatr 2024; 50: 72.
24. Han D, Zhao Z, Mao T, et al. Ginsenoside Rg1: a neuroprotective natural dammarane-type triterpenoid saponin with anti-depressive properties. CNS Neurosci Ther 2024; 30: e70150.
25. Zhu Y, Zou W, Sun B, et al. Ginsenoside Rg1 regulates the activation of astrocytes through lncRNA-Malat1/miR-124-3p/Lamc1 axis driving PI3K/AKT signaling pathway, promoting the repair of spinal cord injury. CNS Neurosci Ther 2024; 30: e70103.
26. Yin S, Xia F, Zou W, et al. Ginsenoside Rg1 regulates astrocytes to promote angiogenesis in spinal cord injury via the JAK2/STAT3 signaling pathway. J Ethnopharmacol 2024; 334: 118531.
27. Parker J, Hockney S, Blaschuk OW, et al. Targeting N-cadherin (CDH2) and the malignant bone marrow microenvironment in acute leukaemia. Expert Rev Mol Med 2023; 25: e16.
28. László ZI, Lele Z. Flying under the radar: CDH2 (N-cadherin), an important hub molecule in neurodevelopmental and neurodegenerative diseases. Front Neurosci 2022; 16: 972059.
29. Guvakova MA, Prabakaran I, Wu Z, et al. CDH2/N-cadherin and early diagnosis of invasion in patients with ductal carcinoma in situ. Breast Cancer Res Treat 2020; 183: 333-46.
30. Situ Y, Deng L, Huang Z, et al. CDH2 and CDH13 as potential prognostic and therapeutic targets for adrenocortical carcinoma. Cancer Biol Ther 2024; 25: 2428469.
31. Liu C, Pan Y, Li Q, et al. Bioinformatics analysis identified shared differentially expressed genes as potential biomarkers for Hashimoto's thyroiditis-related papillary thyroid cancer. Int J Med Sci 2021; 18: 3478-87.
32. Costa P, Rusconi S, Mavilio D, et al. Differential disappearance of inhibitory natural killer cell receptors during HAART and possible impairment of HIV-1-specific CD8 cytotoxic T lymphocytes. AIDS 2001; 15: 965-74.
33. Filaci G, Rizzi M, Setti M, et al. Non-antigen-specific CD8(+) T suppressor lymphocytes in diseases characterized by chronic immune responses and inflammation. Ann N Y Acad Sci 2005; 1050: 115-23.
34. Murdaca G, Spanò F, Contatore M, Guastalla A, Magnani O, Puppo F. Pharmacogenetics of etanercept: role of TNF-α gene polymorphisms in improving its efficacy. Expert Opin Drug Metab Toxicol 2014; 10: 1703-10.
35. Murdaca G, Gulli R, Spanò F, et al. TNF-α gene polymorphisms: association with disease susceptibility and response to anti-TNF-α treatment in psoriatic arthritis. J Invest Dermatol 2014; 134: 2503-9.